GEOPHYSICAL RESEARCH LETTERS, VOL. 36, L08602, doi:10.1029/2008GL036924, 2009

Intensified decadal variability in tropical climate during the late 19th century

Toby R. Ault,[1] Julia E. Cole,[1,2] Michael N. Evans,[1,2,3] Heidi Barnett,[1] Nerilie J. Abram,[4] Alexander W. Tudhope,[5] and Braddock K. Linsley[6]

Received 5 December 2008; accepted 23 January 2009; published 21 April 2009.

[1] To evaluate and extend the record of decadal climate variability, we present a synthesis of 23 coral oxygen isotope records from the tropical Indo-Pacific that extends back to A.D. 1850. Principal components analysis (PCA) on detrended records reveals a leading pattern of variance with significant interannual (3–5 year) and decadal (9–14 year) variability. The temporal evolution and spatial pattern of this variability closely resembles the El Niño/Southern Oscillation (ENSO) pattern across both time scales, suggesting that this decadal tropical variability is fundamentally related to ENSO. The 19th century experienced stronger decadal tropical climate variability, compared to the 20th. Decadal variability in the tropical oceans thus remains underestimated by analysis of direct observations. **Citation:** Ault, T. R., J. E. Cole, M. N. Evans, H. Barnett, N. J. Abram, A. W. Tudhope, and B. K. Linsley (2009), Intensified decadal variability in tropical climate during the late 19th century, *Geophys. Res. Lett.*, *36*, L08602, doi:10.1029/2008GL036924.

1. Introduction

[2] In the tropical Pacific, unstable interactions between sea surface temperature (SST) and the atmosphere generate interannual (2–7 year) El Niño/Southern Oscillation (ENSO) climate anomalies with a characteristic spatial pattern. The Pacific also exhibits variability on decadal (8–14 year) [*White et al.*, 2003; *Tourre and White*, 2006] to multidecadal (20–40 year) [*Mantua et al.*, 1997; *Garreaud and Battisti*, 1999; *Zhang et al.*, 1997] timescales with a similar pattern. Further evidence of decadal variability in the tropical Pacific appears in proxy climate data [*Urban et al.*, 2000; *Cobb et al.*, 2001; *Holland et al.*, 2007].

[3] Previous work has proposed diverse physical mechanisms to explain low-frequency variability (see reviews by *Latif* [1998] and *Mestas-Nuñez and Miller* [2006]). These mechanisms include: physical transport of mid-latitude SST anomalies into the equatorial eastern Pacific [e.g., *Gu and Philander*, 1997; *Luo and Yamagata*, 2001]; wind-driven oceanic Rossby waves that reflect into the thermocline at the western boundary [*White et al.*, 2003]; and autocorrelation arising from oceanic processes driven partly by ENSO variability [e.g., *Newman et al.*, 2003; *Power and Colman*, 2006].

[4] Observational studies of Pacific decadal variability are complicated by the brevity of the instrumental record, which is sparse before the mid-20th century [*Kaplan et al.*, 1998; *Mestas-Nuñez and Miller*, 2006] (Figure 1b), and by the potential for recent anthropogenic influence. To understand decadal variability more fully, we must turn to proxy data. Here we use a new network of 23 coral oxygen isotope ($\delta^{18}O$) records to describe the spectrum of tropical SST in greater detail.

2. Data

[5] Coral records closely track tropical Indo-Pacific variability on interannual to decadal timescales [*Urban et al.*, 2000; *Cobb et al.*, 2001; *Linsley et al.*, 2008]. In warmer and/or lower salinity conditions (e.g., from precipitation or freshwater flux), corals incorporate less of the heavy isotope of oxygen (^{18}O) into their skeletons, driving $\delta^{18}O$ values lower. The inverse relationship between $\delta^{18}O$ and both precipitation amount and SST in tropical locales allows SST reconstructions spanning several centuries (as summarized by *Cole* [2003] and *Lough* [2004]). On interannual timescales, researchers have demonstrated that large-scale patterns of tropical SST covariability (e.g., ENSO) can be reliably reconstructed from a limited number of records [*Evans et al.*, 2002; *Wilson et al.*, 2006]. On decadal timescales, low signal to noise ratios present greater challenges to pattern identification [*Lough*, 2004; *Linsley et al.*, 2008], but analysis of a network of sites can expose common patterns. We use this coral network-based approach to identify large-scale patterns of decadal variability that emerge from proxy and instrumental records.

[6] We use 23 coral $\delta^{18}O$ records from the Indian and Pacific Oceans in our synthesis (Table S1 of the auxiliary material), including only sites with $\geq$90% of the 1850–1990 interval to minimize non-stationarity.[1] We converted each subannually-resolved time series into a yearly average using the May-April year to emphasize the seasonal expression of El Niño/La Niña conditions [*Rasmusson and Carpenter*, 1982]. We made no adjustments to existing annual records. Because many coral records have trends that do not unequivocally reflect climate [see *Lough*, 2004], we detrended all

[1]Department of Geosciences, University of Arizona, Tucson, Arizona, USA.
[2]Department of Atmospheric Sciences, University of Arizona, Tucson, Arizona, USA.
[3]Laboratory of Tree Ring Research, University of Arizona, Tucson, Arizona, USA.
[4]British Antarctic Survey, Natural Environment Research Council, Cambridge, UK.
[5]School of GeoSciences, University of Edinburgh, Edinburgh, UK.
[6]Department of Earth and Atmospheric Sciences, State University of New York at Albany, Albany, New York, USA.

0094-8276/09/2008GL036924$05.00

[1]Auxiliary materials are available in the HTML. doi:10.1029/2008GL036924.

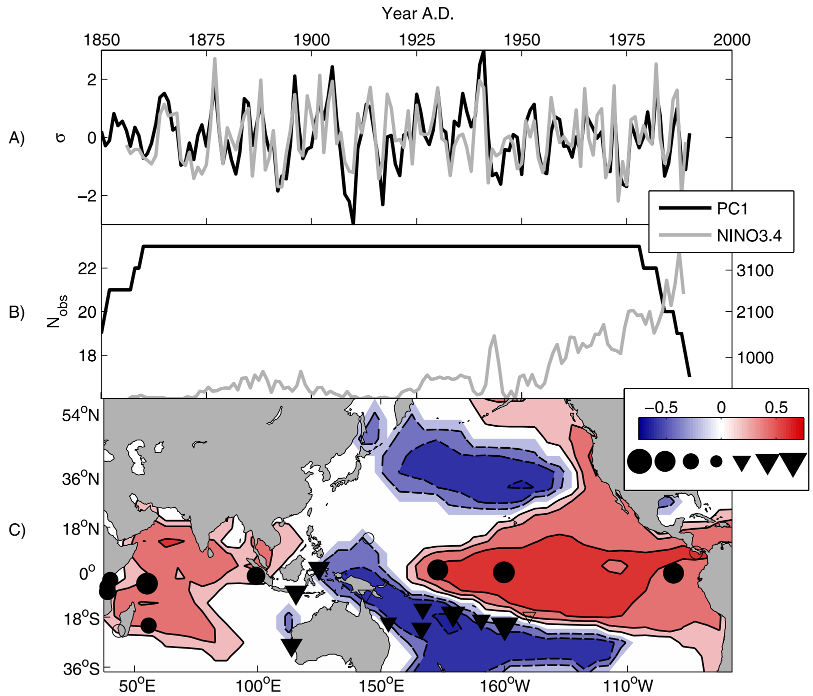

Figure 1. (a) First (rotated) principal component of the 23 coral records, (black line), plotted with the Niño3.4 SST index (grey line). (b) Number of records that contribute to our coral synthesis (black line, left axis). Grey line indicates the average number of instrumental SST measurements during the May to April year in the NINO3.4 region. (c) Map shows correlation of the first principal component of coral data with instrumental SST (colored at the 95% confidence level) and with individual detrended δ^{18}O records (symbols; filled indicate 95% confidence). Red areas and circles indicate warm SST and more negative δ^{18}O values, respectively, during El Niño events. Blue areas and triangles indicate cool SST and less negative δ^{18}O values during El Niño events.

annualized records using a spline to remove $\geq$50% of the variance at periods $\geq$100 years. Detrending did not alter the spectrum of any individual record at the timescales discussed here. We performed a parallel analysis on instrumental SST anomalies for 1901–1990 in the Pacific and Indian Oceans (5×5 resolution) and on an index of central Pacific SST anomalies (NINO3.4) [*Kaplan et al.*, 1998], using the same May-April year.

3. Methods

[7] To assess network-wide patterns of spatiotemporal variability, we performed principal component analysis (PCA) on the annualized, detrended δ^{18}O time series using the correlation matrix. We apply the same analysis to instrumental SST records from the location of each coral record. We determined the spatial expression of each principal component time series (PC) by correlating it with each of the annualized, detrended coral records and with the gridded SST dataset. We established confidence limits for the leading eigenmodes using a Monte Carlo (rule N) significance test [*Preisendorfer et al.*, 1988] modified for autocorrelation.

[8] To detect patterns of low-frequency variability in the leading principal component (PC1) and in individual δ^{18}O records, we applied two complementary methods of spectral analysis: the multi-taper method (MTM) [*Thomson*, 1982] and singular spectrum analysis (SSA) [*Ghil et al.*, 2002]. We used a Monte Carlo approach to test the significance of each signal identified by MTM and SSA against a red-noise null hypothesis [*Ghil et al.*, 2002].

[9] We applied SSA to PC1 and identified significant decadal variability. Next we used SSA to extract decadal (8–15 year) components, where present, from each of the δ^{18}O and SST series. Finally, we correlated the decadal δ^{18}O and SST fields with the decadal component derived from the PCA. To assess the significance of correlations between reconstructed decadal components from SSA, we estimate the effective degrees of freedom by 2*N/M, where N is the length of the time series and M is the SSA window length, which yields 19 effective degrees of freedom in the filtered coral records and 12 degrees of freedom in the filtered SST records. Effective degrees of freedom for non-zero lags are estimated by N/M (9.4 for δ^{18}O, 6 for SST). The 95% confidence limits obtained using this approach were slightly more conservative than those derived from a Monte Carlo approach.

4. Results

[10] Results of PCA are shown in Figure 1. PC1 correlates significantly with the NINO3.4 index ($r = -0.71$; $p < 0.001$). Spatially, PC1 correlates with annual SST anomalies in approximately the canonical ENSO pattern. Individual coral records correlate with PC1 according to their location with respect to the canonical ENSO pattern (Figure 1c).

[11] In addition to interannual variance associated with ENSO, spectral analysis suggests the importance of decadal

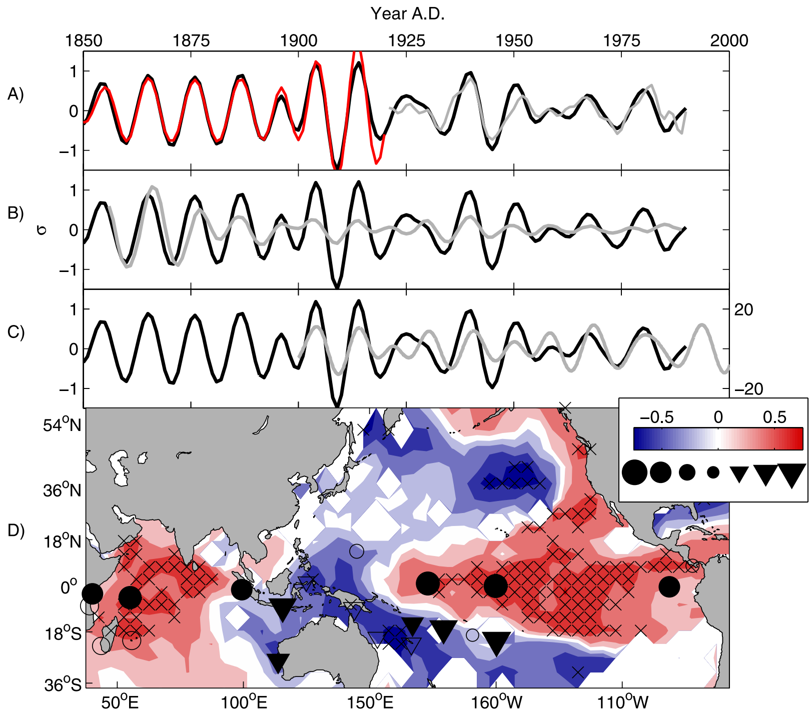

Figure 2. Estimates of the PC1 decadal signal from 1850–1990 (black line) shown with: (a) the 1850–1920 (red line) and 1921–1990 (grey line) signal estimates; (b) the decadal reconstructed component from Niño3.4 (grey line); (c) the "quasi-decadal" signal in instrumental SST records (grey line) [*Tourre and White*, 2006]. (d) Same as for Figure 1c, but using the decadally filtered versions of the PC1, SST (hatched where significant at the 95% confidence level), and coral δ^{18}O records.

variability in PC1 (Figure S1). Monte Carlo SSA (Table 1) identifies a significant decadal (9–14 yr) component that explains 36% of the variance in PC1 (Figure 2). Seasonal analysis of the high-resolution records (Figure S3) identifies the boreal winter and fall (SON and DJF) as the times of greatest amplitude in this signal. PCA performed on the SST records from the individual coral sites reveals this same signal (results not shown).

[12] The decadal component appears stronger from 1850–1920 than from 1920–1990. To test this observation, we partitioned PC1 into two time series of near-equal length (1850–1920 and 1921–1990) and applied SSA to each interval. From 1850–1920 the decadal signal is significant at the 95% confidence level and explains 51% of the variance; after ~1920, it explains 11% of the variance and is not significant (Table 1). Singular values corresponding to the decadal components are larger during the earlier interval (Table 1), meaning that the absolute strength of the signal is greater from 1850–1920 than from 1921–1990. Wavelet analysis of PC1 and other long ENSO indices (e.g., the SOI) confirms that the earlier interval experiences enhanced decadal variability (Figure S2).

[13] Decadal components from 11 out of 23 sites correlate significantly ($P_{adj} < 0.05$) with the PC1 decadal signal (Figure 2d and Table S1). Positive correlations occur in the equatorial Pacific and Indian Ocean; negative values occur primarily in the south Pacific, Indonesia, and eastern Indian Ocean. The decadal component from PC1 correlates negatively with decadal SST from much of the tropical Indo-Pacific, and positively with decadal SST from the extra-tropical Pacific (Figure 2d, colors). Overall, the spatial pattern of correlation with PC1 is similar for both SST and δ^{18}O records, across interannual and decadal time scales. However, the decadal pattern is displaced to the west of the canonical ENSO pattern and lacks power in the eastern equatorial and subtropical Pacific. We do not find evidence for propagation of decadal

Table 1. Summary of SSA Performed on the Leading Principal Component of the Coral Network for the Intervals Indicated Above and on the NINO3.4 Series[a]

Time Series (and Interval)	Signal (and RC Rank)	Timescale	Variance (Singular Value/M)
PC1 (1850–1990)	Decadal (1–2)**	9–13yr	35.9% (0.22)
	ENSO (3–4)**	5–6yr	20.97% (0.17)
PC1 (1850–1920)	Decadal (1–2)**	9–10yr	51.2% (0.26)
	ENSO (5–6)	3–6yr	9.42% (0.11)
PC1 (1921–1990)	Decadal (3–4)	~14yr	10.9% (0.08)
	ENSO (1–2)**	5–6yr	31.5% (0.27)
NINO3.4 (1857–1990)	ENSO (1–4, 7–8)**	3–6yr	36.28% (0.26)
	Decadal (5–6)**	9–12yr	10.97% (0.11)

[a]Total fraction of variance explained by each RC and its corresponding singular value (in parentheses) normalized by the window length (M).

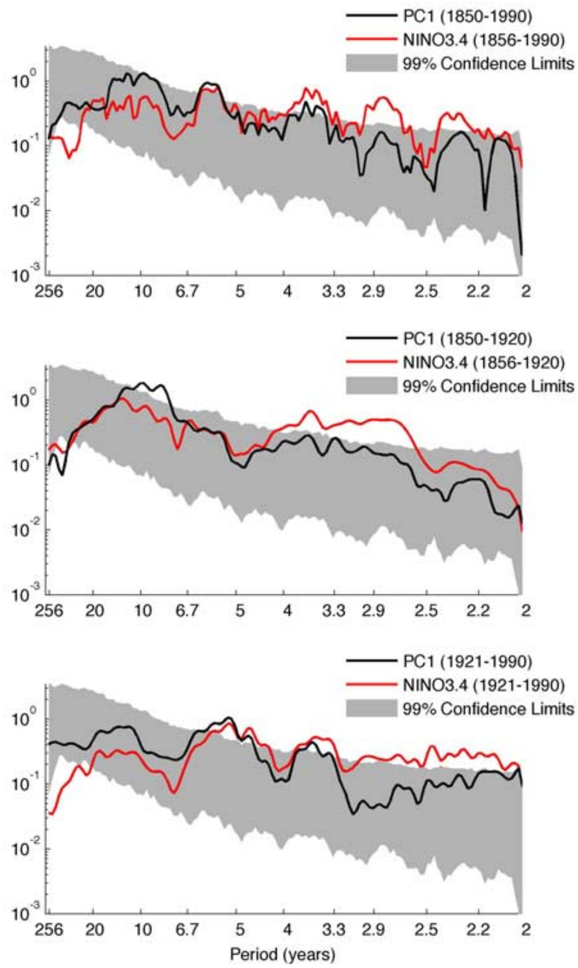

Figure 3. Spectra of the PC1 time series from (top) 1850–1990, (middle) 1850–1920 and (bottom) 1921–1990. In each plot the red line shows the PC1 spectra for the given interval and the black line shows the NINO3.4 spectrum for the entire 1854–1990 interval. The grey shading indicates the 99% confidence bounds from 1000 Monte Carlo realizations of a red noise time series with the same correlation with NINO3.4 and autocorrelative properties (AR(1)) as the PC1 time series [e.g., *Newman et al.*, 2003].

signals. Instead, maximum correlations occur within a one-year lag (Table S1), within the age uncertainty of most coral records.

[14] Age model uncertainties in the proxy data, detrending and PCA choices (e.g., between correlation and covariance matrix) made little or no difference in the spatial pattern or time series of the decadal signal. However, age model errors are likely to be cumulative further back in time and hence may blur interannual signals while retaining long-period variance. Additional Monte Carlo analysis suggests that this effect could damp high frequency components earlier in time, but it is inconsistent with the late 19th enhancement of decadal variability. First, the corals show changes in *absolute* magnitude of the decadal signal; age model error could attenuate signals, especially at higher frequencies, but it cannot enhance variance. Second, most individual records that contain the PC1 decadal signal also exhibit intensification earlier in time (Table 1); age model-related damping should operate strongly only when records are combined. Finally, instrumental records, which are not subject to age-model errors, show the same pattern.

5. Discussion

[15] We show that the 9–14 year signal in corals is highly significant during the 19th century and is present (weakly) during the 20th. We therefore argue that tropical decadal variability is more important than inferred from 20th century instrumental records alone. The spatial and temporal similarities of the decadal signal to the 2–7 year ENSO component suggest that the physical mechanisms may also be similar.

[16] Comparing decadal statistics of PC1 with the NINO3.4 index highlights an important contrast between our results and instrumental estimates of tropical decadal variability. Overall, decadal variability only accounts for 11% of the total variance in the NINO3.4 SST series whereas in PC1 from the coral network, it makes up 36% of the total variance. This discrepancy likely reflects the importance of the decadal component over time and is not a bias of the geographic distribution of corals, as the network of SST records also exhibit this pattern with an enhanced (albeit slightly) decadal component during the late 19th century.

[17] We interpret the enhanced decadal variability seen in the coral network and the NINO3.4 region as evidence of greater ENSO-like tropical decadal variability during the late 19th century, when instrumental data are sparse. Further support comes from the Maiana Atoll [*Urban et al.*, 2000] and Jarvis Island records, which are located within the NINO3.4 region and show a clear intensification of decadal variability during the late 19th century. The strong DJF seasonality, spatial pattern, and correlation field with SST all support this interpretation. Finally, additive contributions of SST and salinity to coral δ^{18}O records could reinforce the decadal signal in corals when it was more energetic further back in time [*Cole et al.*, 1993; *Guilderson and Schrag*, 1999; *Urban et al.*, 2000; *Linsley et al.*, 2008].

[18] Any physical mechanism used to explain enhanced variance in the decadal pattern during the late 19th century must also explain the boreal winter enhancement, the roughly simultaneous evolution of the spatial pattern of SST anomalies, and the time-varying amplitude. We argue that solar forcing is unlikely to drive this decadal variability, because of the near-180° phase reversal between sunspot maxima and the decadal signal over the course of our record (Figure S4). Between 1850 and 1900, sunspot number (SSN) maxima are approximately 180° out of phase with El Niño-like conditions in the network of corals, whereas at the end of the 20th century SSN maxima are in phase with El Niño-like conditions.

[19] Could random changes in the tropical Pacific ocean-atmosphere system, combined with memory in the ocean mixed layer [e.g., *Power and Colman*, 2006; *Newman et al.*, 2003] produce decadal ENSO-like variability? To test this null hypothesis, we use a stochastic linear model [*Newman et al.*, 2003] to realize 1000 Monte Carlo time series with the same autocorrelative properties and relationship with ENSO as our PC1. The spectra of these realizations (Figure 3) suggest that we cannot rule out this null hypothesis of

decadal variability after 1920. However, between 1850–1920 decadal variance in PC1 is outside the stochastic model's 99% confidence limit. This finding suggests that either additional processes may be needed to explain the strength of tropical decadal variability during the late 19th century [e.g., *Luo and Yamagata*, 2001; *White et al.*, 2003], or that changes in ENSO variability may be modified through ocean processes [e.g., *Power and Colman*, 2006] that intensify decadal variability at the edge of the ENSO system where many of the coral records are located. In either case, future work should focus on determining which mechanisms could exhibit such non-stationarity in decadal variance.

6. Conclusions

[20] We identify a strong decadal component of climate variability in a network of 23 coral δ^{18}O records from 1850 to 1990. This signal closely matches instrumental results from the 20th century [*Tourre and White*, 2006] and extends the record into a period of much stronger decadal variance in the 19th century. Seasonal analyses indicate that the decadal mode is stronger in boreal fall/winter than in spring/summer. In the coral network the spatial pattern of this mode is very similar to interannual ENSO variability. The correlation field of the decadal coral signal with decadal SST identifies the central Pacific as the center of action, and implies the pattern is displaced to the west of the canonical ENSO pattern. Given the spatial pattern, seasonality, and strength of the signal, we infer that this decadal signal represents a fundamental timescale of ENSO variability, whose enhanced variance in the late 19th century remains to be explained.

[21] **Acknowledgments.** We thank Andrew C. Comrie, Tom D. Damassa, Michael E. Mann, Joellen L. Russell, Jonathan T. Overpeck, and Vikram Mehta for helpful comments and support on this project. We also appreciate the assistance of Yves M. Tourre, Warren B. White and Ted Walker who kindly shared data from their analysis of instrumental sea surface temperature records. This research was supported by NOAA's Paleoclimatology program (OAR/CCDD grant NA03OAR4310152 to JEC), NSF/ATM03 (grant 49356 to MNE), and the NSF graduate research fellowship program (to T. Ault).

References

Cobb, K. M., C. D. Charles, and D. E. Hunter (2001), A central tropical Pacific coral demonstrates Pacific, Indian, and Atlantic decadal climate connections, *Geophys. Res. Lett.*, *28*(11), 2209–2212.

Cole, J. E. (2003), Holocene coral records: Windows on tropical climate variability, in *Global Change in the Holocene*, edited by A. McKay et al., pp. 168–184, Arnold, London.

Cole, J. E., R. G. Fairbanks, and G. T. Shen (1993), Recent variability in the Southern Oscillation: Isotopic results from a Tarawa Atoll coral, *Science*, *260*(5115), 1790–1793.

Evans, M. N., A. Kaplan, and M. A. Cane (2002), Pacific sea surface temperature field reconstruction from coral δ^{18}O data using reduced space objective analysis, *Paleoceanography*, *17*(1), 1007, doi:10.1029/2000PA000590.

Garreaud, R. D., and D. S. Battisti (1999), Interannual (ENSO) and interdecadal (ENSO-like) variability in the Southern Hemisphere tropospheric circulation, *J. Clim.*, *12*(7), 2113–2123.

Ghil, M., et al. (2002), Advanced spectral methods for climatic time series, *Rev. Geophys.*, *40*(1), 1003, doi:10.1029/2000RG000092.

Gu, D. F., and S. G. H. Philander (1997), Interdecadal climate fluctuations that depend on exchanges between the tropics and extratropics, *Science*, *275*(5301), 805–807.

Guilderson, T. P., and D. P. Schrag (1999), Reliability of coral isotope records from the western Pacific warm pool: A comparison using age-optimized records, *Paleoceanography*, *14*(4), 457–464.

Holland, C. L., R. B. Scott, S. I. An, and F. W. Taylor (2007), Propagating decadal sea surface temperature signal identified in modern proxy records of the tropical Pacific, *Clim. Dyn.*, *28*(2–3), 163–179.

Kaplan, A., M. A. Cane, Y. Kushnir, A. C. Clement, M. B. Blumenthal, and B. Rajagopalan (1998), Analyses of global sea surface temperature 1856–1991, *J. Geophys. Res.*, *103*(C9), 18,567–18,589.

Latif, M. (1998), Dynamics of interdecadal variability in coupled ocean-atmosphere models, *J. Clim.*, *11*(4), 602–624.

Linsley, B. K., P. Zhang, A. Kaplan, S. S. Howe, and G. M. Wellington (2008), Interdecadal-decadal climate variability from multicoral oxygen isotope records in the South Pacific Convergence Zone region since 1650 A.D., *Paleoceanography*, *23*, PA2219, doi:10.1029/2007PA001539.

Lough, J. M. (2004), A strategy to improve the contribution of coral data to high-resolution paleoclimatology, *Palaeogeogr. Palaeoclimatol. Palaeoecol.*, *204*(1–2), 115–143.

Luo, J.-J., and T. Yamagata (2001), Long-term El Niño-Southern Oscillation (ENSO)-like variation with special emphasis on the South Pacific, *J. Geophys. Res.*, *106*(C10), 22,211–22,227.

Mantua, N. J., S. R. Hare, Y. Zhang, J. M. Wallace, and R. C. Francis (1997), A Pacific interdecadal climate oscillation with impacts on salmon production, *Bull. Am. Meteorol. Soc.*, *78*(6), 1069–1079.

Mestas-Nuñez, A. M., and A. J. Miller (2006), Interdecadal variability and climate change in the eastern tropical Pacific: A review, *Prog. Oceanogr.*, *69*(2–4), 267–284.

Newman, M., G. P. Compo, and M. A. Alexander (2003), ENSO-forced variability of the Pacific decadal oscillation, *J. Clim.*, *16*(23), 3853–3857.

Power, S., and R. Colman (2006), Multi-year predictability in a coupled general circulation model, *Clim. Dyn.*, *26*(2–3), 247–272.

Preisendorfer, R. W., C. D. Mobley, and T. P. Barnett (1988), The Principal Discriminant Method of prediction: Theory and evaluation, *J. Geophys. Res.*, *93*(D9), 10,815–10,830.

Rasmusson, E. M., and T. Carpenter (1982), Variations in tropical sea surface temperature and surface winds associated with the Southern Oscillation/El Niño, *Mon. Weather Rev.*, *110*, 354–384.

Thomson, D. J. (1982), Spectrum estimation and harmonic-analysis, *Proc. IEEE*, *70*(9), 1055–1096.

Tourre, Y. M., and W. B. White (2006), Global climate signals and equatorial SST variability in the Indian, Pacific and Atlantic oceans during the 20th century, *Geophys. Res. Lett.*, *33*, L06716, doi:10.1029/2005GL025176.

Urban, F. E., J. E. Cole, and J. T. Overpeck (2000), Influence of mean climate change on climate variability from a 155-year tropical Pacific coral record, *Nature*, *407*(6807), 989–993.

White, W. B., Y. M. Tourre, M. Barlow, and M. Dettinger (2003), A delayed action oscillator shared by biennial, interannual, and decadal signals in the Pacific Basin, *J. Geophys. Res.*, *108*(C3), 3070, doi:10.1029/2002JC001490.

Wilson, R., A. Tudhope, P. Brohan, K. Briffa, T. Osborn, and S. Tett (2006), Two-hundred-fifty years of reconstructed and modeled tropical temperatures, *J. Geophys. Res.*, *111*, C10007, doi:10.1029/2005JC003188.

Zhang, Y., et al. (1997), ENSO-like interdecadal variability: 1900–93, *J. Clim.*, *10*(5), 1004–1020.

N. J. Abram, British Antarctic Survey, Natural Environment Research Council, High Cross, Madingley Road, Cambridge CB3 0ET, UK.

T. R. Ault, H. Barnett, J. E. Cole, and M. N. Evans, Department of Geosciences, University of Arizona, 1040 East 4th Street, Tucson, AZ 95721, USA. (tault@geo.arizona.edu)

B. K. Linsley, Department of Earth and Atmospheric Sciences, State University of New York at Albany, 1400 Washington Avenue, Albany, NY 12222, USA.

A. W. Tudhope, School of GeoSciences, University of Edinburgh, West Mains Road, Edinburgh EH9 3JW, UK.